Journal of Zhejiang University-SCIENCE A (Applied Physics & Engineering)
ISSN 1673-565X (Print); ISSN 1862-1775 (Online)
www.zju.edu.cn/jzus; www.springerlink.com
E-mail: jzus@zju.edu.cn

Effects of vacancies on interwall spacings of multi-walled carbon nanotubes*

Ming-du MA[1], Jefferson Zhe LIU[†‡2], Li-feng WANG[3], Lu-ming SHEN[4], Quan-shui ZHENG[†‡1]
([1]Department of Engineering Mechanics, Tsinghua University, Beijing 100084, China)
([2]Department of Mechanical and Aerospace Engineering, Monash University, Clayton, Victoria 3168, Australia)
([3]Department of Mechanical Engineering, Massachusetts Institute of Technology, Cambridge, Massachusetts 02139, USA)
([4]School of Civil Engineering, University of Sydney, NSW 2006, Australia)
[†]E-mail: jzliu@eng.monash.edu.au; zhengqs@tsinghua.edu.cn
Received Apr. 16, 2010; Revision accepted July 22, 2010; Crosschecked Sept. 16, 2010

Abstract: We use molecular dynamics (MD) simulations to study the effects of vacancies on tube diameters and interwall spacings of multi-walled carbon nanotubes (MWCNTs). Two types of vacancies, double vacancy and three dangling-bond (3DB) single vacancy, are identified to have opposite effects on the tube size change, which explains the inconsistency of the experimentally measured interwall spacings of MWCNTs after electron beam irradiation. A theoretical model to quantitatively predict the shrunk structures of the irradiated MWCNTs is further developed. We also discuss the fabrications of prestressed MWCNTs, in which reduced interwall spacings are desired to enhance the overall elastic modulus and strength.

Key words: Multi-walled carbon nanotubes (MWCNTs), Noise carbon nanotubes, Electron beam irradiation, Defects
doi:10.1631/jzus.A1000174 **Document code:** A **CLC number:** TB383

1 Introduction

Pristine single-walled carbon nanotubes (SWCNTs) have extremely high values of both axial Young's moduli (about 1 TPa) and tensile strengths (70–100 GPa) compared with all other existing materials (Mielke *et al.*, 2007). However, the measured values of the overall axial Young's modulus and strength of multi-walled carbon nanotubes (MWCNTs) are found to be one or even more orders of magnitude lower than those of SWCNTs (Yu *et al.*, 2000a; 2000b; Ding *et al.*, 2007). This low elastic modulus and strength are mainly caused by the ultra-low interwall shear strength, which ranges from 0.08 to 0.3 GPa (Cumings and Zettl, 2000; Yu *et al.*, 2000a; 2000b) and thus prevents the axial tensile loadings exerted on the outer surface of an individual MWCNT from being effectively transferred to the inner tubes.

Prestressed multi-walled carbon nanotubes (PMWCNTs) were recently proposed by Xu *et al.* (2008) as a solution to enhance the interwall shear strength of an MWCNT by several orders of magnitude, without reducing its tensile strength or tensile stiffness. A PMWCNT is composed of coaxial SWCNTs with interwall spacings smaller than those of normal MWCNTs, e.g., about 0.34 nm. Atomic simulations showed that, for instance, a PMWCNT with 20% reduction in interwall spacings could lead to an enhancement of its interwall shear strength up to four orders of magnitude and a consequent 20% or so enhancement of its overall axial Young's modulus and strength (Xu *et al.*, 2008). However, 20% reduction of

‡ Corresponding authors
* Project supported by the National Basic Research Program (973) of China (No. 2007CB936803), the National High-Tech R&D Program (863) of China (No. 2008AA03Z302), the National Natural Science Foundation of China (No. 10832005), and the Joint Research Scheme of the National Natural Science Foundation of China and Research Grants Council of Hong Kong (No. 50518003)

the interwall spacing leads to 100 GPa self-balanced interwall pressure, which will prohibit fabrication of PMWCNTs with the techniques to date. Experimental results in (Banhart and Ajayan, 1996; Sun *et al.*, 2006; Sun *et al.*, 2008) reported that the as-grown diameters of MWCNTs and the interwall distance of MWCNTs and carbon onions (e.g., about 0.34 nm) can be altered by electron beam irradiation at ambient pressure and 500–600 °C. Similar size shrinkage of SWCNTs caused by electron beam irradiation has also been observed (Ajayan *et al.*, 1998).

2 Experimental

To experimentally verify some theoretical predictions of PMWCNTs (Xu *et al.*, 2008), we performed similar irradiation-high temperature experiments on Fe_3C-filled MWCNTs. The Fe_3C-filled MWCNTs were synthesized by catalytic decomposition of 0.06 g/ml ferrocene in dichlorobenzene solution in a quartz tube, with the reaction temperature of 860 °C and the gas flowing rates of 2000 and 300 ml/min for Ar and H_2 respectively. After the furnace cooling down in argon atmosphere to room temperature, the macroscopic carbon nanotube (CNT) films were collected from the interior wall of the quartz, and then sonicated in ethanol and deposited onto labeled metal grids with carbon membrane for using in TEMs. Fig. 1a shows the transmission electron microscope (TEM) image of an as-grown Fe_3C-filled MWCNT at room temperature. The specimen was then irradiated at a beam current density of 6 A/cm^2 for 19 min under 500 °C within a second TEM (JEM 1000, JEOL, Tokyo, Japan) operated at 750 kV. Next, we kept the sample in vacuum at 500 °C for 5 min after the irradiation, and subsequently cooled it down to the ambient temperature. The irradiated specimen was then put back into the first TEM (JEM 2011, JEOL, Tokyo, Japan) operated at 200 kV, ambient temperature, and current density about 100 A/cm^2 for about 1 min to obtain the image as shown by Fig. 1b. Careful inspection of Figs. 1a and 1b indicates a 27.2% diameter shrinkage of the Fe_3C core (black parts in the images).

The deformation of the Fe_3C core is a consequence of the shrinkage of the surrounding MWCNT, as indicated in Sun *et al.* (2006). Because the samples

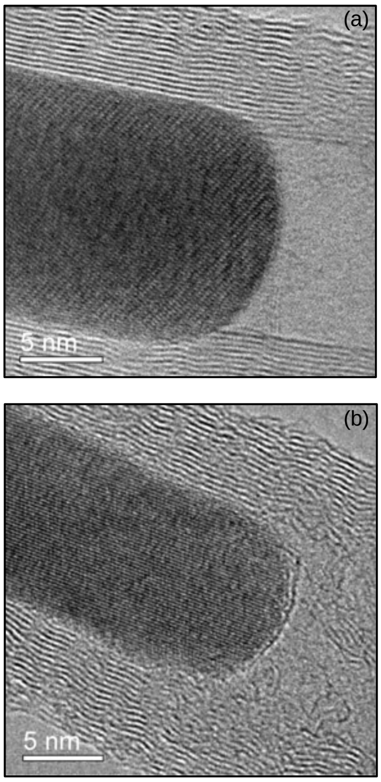

Fig. 1 An as-grown Fe_3C-filled MWCNT sample observed in TEM (JEM 2011) at room temperature
(a) The image of the same MWCNT after electron beam irradiation in TEM (JEM 1000); (b) The diameter of the Fe_3C core (black in (a) and (b)) was reduced by 27.2% after the irradiation

and temperature used in our experiments are similar to those in Sun *et al.* (2006), the MWCNT should provide a pressure up to 40 GPa to exceed the plastic flow stress of the Fe_3C core as in Sun *et al.* (2006). They also observed a significant reduction of interwall spacing of the two innermost walls down to 0.29–0.31 nm, which was attributed to the high pressure exerted on the innermost walls. We also measured the interwall spacings of our irradiated sample. Much to our surprise, however, the interwall spacings of the innermost walls were measured close to those of the as-grown MWCNT, without a notable shrinkage observed.

3 Atomic simulations

Interwall spacing is a critical structural parameter of PMWCNTs. It is crucial to understand what results in this experimental controversy, which may prevent fabrication of PMWCNTs. In this study, we systematically investigate the effects of different defects on the tube diameter using molecular dynamics (MD) simulations. We found that the three dangling-bond (3DB) single vacancy (SV) has an effect opposite to that of the double vacancy (DV) on changing of the tube diameter, and that it was the interplay of these two kinds of defects, which were generated by the electron beam irradiation at different temperatures respectively, resulted in different experimental observations. Based on this understanding, we propose a model to predict the equilibrium structure of the irradiated MWCNT (PMWCNT) from given experimental irradiation conditions. Finally, we discuss some key issues regarding fabrication of PMWCNTs.

In the irradiation experiments, the acceleration voltage of TEM is usually much higher than the threshold voltage for knocking off atom from graphite, namely 86 kV or even less for CNT (Krasheninnikov and Banhart, 2007; Krasheninnikov *et al.*, 2007), and atomic defects will thus be generated in CNTs. In experiments, 3DB SV has been observed (Hashimoto *et al.*, 2004). Theoretical calculations show that there are other defects which are more stable than 3DB SV, such as DV and 5-1 dangling bond (5-1DB) SV. It is believed that the existence of the defects induced the observed shrinkage of CNTs and carbon onions (Zaiser, 1999; Sun *et al.*, 2006). Using tight-binding calculations, Sun *et al.* (2006) found that DV caused shrinkage of the diameters and reduction of interwall spacings of CNTs. Here we used the second-generation reactive empirical bond order (REBO) potential with its extension (Stuart *et al.*, 2000), and software package LAMMPS (large-scale atomic/molecular massively parallel simulator) (Plimpton, 1995) for the MD simulations to investigate the influences of different defects on the interwall spacings of MWCNTs.

We carried out atomic simulations of a (5,5)@(10,10) double-walled carbon nanotube (DWCNT) and a (10,10) SWCNT, with periodic boundary conditions in axial direction for a 5-nm long supercell. It is assumed that, during the simulations, the (5,5) inner tube had no deformation to model the constraint of the stiff Fe_3C core. Three types of defects were considered: DV, 3DB SV and 5-1DB SV. The defects were generated randomly on the (10,10) CNTs and then the atomic positions were relaxed in MD simulations. Fig. 2 illustrates the calculated equilibrium diameters of the (10,10) CNTs D as a function of knocked-off atom density n. We can see that with DV or 5-1DB SV, D decreases linearly as n increases. In contrast, 3DB SV has the opposite effect: D increases linearly with increase of n (Fig. 2). The linear dependence can be modeled by

$$D=(1-kn)D_0, \tag{1}$$

where D_0 is the diameter of the defect-free CNTs. The simulated linear dependence of D on DV density, k=0.68, agrees very well with the density functional theory based tight-binding (DFTB) simulation results (Sun *et al.*, 2006).

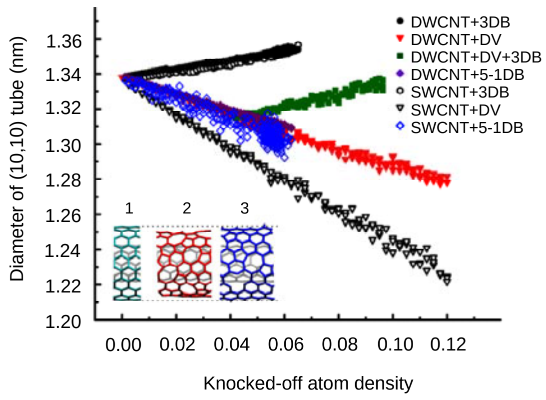

1: Atomic structure of a defect-free DWCNT;
2: Atomic structure of a DWCNT with DVs at n=0.12;
3: Atomic structure of a DWCNT with both DVs and 3DB SVs at n=0.04

Fig. 2 Diameter of (10,10) tube of the energy optimized structures of a (5,5)@(10,10) DWCNT and a (10,10) SWCNT with different knocked-off atom densities

We may describe the physical processes of the irradiation experiments as follows. During irradiation, an electron beam would first knock off carbon atoms from a nanotube individually to generate the so-called ideal SVs (Wang and Wang, 2006). Ideal SVs would then either reconstruct to form either 3DB (Hashimoto *et al.*, 2004; Wang and Wang, 2006) or 5-1DB SVs (Lu and Pan, 2004), or each two migrate to form a DV (Krasheninnikov *et al.*, 2006). DV is the most stable among the three types of defects, and at a temperature of 100 °C or above the thermal energy can activate migration of SVs to form DVs (Krasheninnikov *et al.*, 2006). In the electron beam irradiation experiments at temperature of 500–600 °C, DVs would be the dominant defects (Sun *et al.*, 2006). Our MD results for DV (Fig. 2) explain the shrinkage of interwall spacing of MWCNT observed in the in situ experiments (Sun *et al.*, 2006).

In contrast to the in situ observations in Sun *et al.* (2006), our samples were exposed to electron beam irradiation twice. The first irradiation was at a temperature of 500 °C and the second was at room temperature during the TEM observation. Not only DVs, but also the 3DB and 5-1DB SVs, would be generated on our samples. Although 5-1DB SV has lower energy than 3DB SV, first-principles calculations (Wang and Wang, 2006) revealed that the critical temperature needed for reconstruction of ideal SVs into 3DB SVs is about −13 °C, while 1200 °C is required for the reconstruction to 5-1DB SVs. Our samples would thus have two types of defects: DV and 3DB SV. We believe that the opposite effects of these two defects on change of the tube diameter (Fig. 2) can explain the different observations of the interwall spacings in various experiments. We further performed MD calculations to simulate the two-step irradiations. The inset and the solid square symbols in Fig. 2 illustrated this process. The DVs were first introduced into the outer wall of a defect-free DWCNT (with the inner wall fixed) and the subsequent relaxation led to reduction of the outer wall diameter. The 3DB SVs were then introduced into the outer wall and then D began to expand linearly with increases in the density n of 3DB SVs. Based on the atom displacement rate relation (Banhart, 1999), the maximal defect density $n_{\max}$ can be estimated as $n_{\max}=\sigma jt$, where σ is the displacement cross section, t the irradiation time, and j the beam current density. With the values of $\sigma\approx 6$ barn (1 barn=10^{-28} m^2) (Zobelli *et al.*, 2007) and j=100 A/cm^2 for radiating CNTs within TEM operated at 200 kV, we obtained $n_{\max}$=0.225 for the 1-min room temperature irradiation. Introduction of 3DB SV with this density will lead to a radial expansion of 10.5% according to the linear dependence in Eq. (1) with k=−0.24 fitted from Fig. 2. This result agrees well with the previous estimation (10%–13%) of the releasing strain (Sun *et al.*, 2006).

4 Continuum model

It is not feasible to predict the diameters of each wall and interwall spacings of an irradiated MWCNT directly from MD simulations. Here we proposed a model instead by incorporating the obtained linear dependence of the equilibrium diameter of an irradiated SWCNT on the DV density of $n/2$ (Fig. 2).

For an MWCNT with a given DV density of $n/2$, ignoring the relatively small bending energy, the total energy of the system Π includes two parts: interwall van der Waals interaction energy density U_v and intrawall elastic energy density U_e:

$$\Pi = \pi s_0 \sum_{i=1}^{N} D_i^s \left(U_\mathrm{v}(\varepsilon_i^r) + U_\mathrm{e}(\varepsilon_i^\theta, n) \right), \tag{2}$$

where N denotes the wall number. For $U_\mathrm{v}(\varepsilon_i^r)$ within the compression range, we adopted

$$U_\mathrm{v}(\varepsilon_i^r) = \kappa \left(\frac{(\varepsilon_i^r)^2}{2} + \alpha \frac{(\varepsilon_i^r)^4}{4} \right), \tag{3}$$

where κ=29 GPa and α=130, as used in Sun *et al.*'s work (Zaiser, 1999; Sun *et al.*, 2006), $\varepsilon_i^r=(D_{i+1}-D_{i-1})/(4s_0)-1$ ($s_0\approx 0.335$ nm) is the interwall strain, D_i is the undetermined equilibrium diameter of the ith wall inside the irradiated MWCNT. The two assistant wall diameters D_0 and D_{N+1} were defined as $D_0=D_1-2s_0$ and $D_{N+1}=D_N+2s_0$, respectively (Zaiser, 1999; Sun *et al.*, 2006). Because irradiation would result in significant shrinking strains (10%–13%), we employed the nonlinear elastic model (Lee *et al.*, 2008):

$$U_\mathrm{e}(\varepsilon_i^\theta, n) = \frac{E(n)(\varepsilon_i^\theta)^2}{2} + \frac{E_2(n)(\varepsilon_i^\theta)^3}{3}, \tag{4}$$

where $E(n)$ and $E_2(n)$ are the Young's modulus and the second order Young's modulus of SWCNT with DV density of $n/2$, respectively, $\varepsilon_i^\theta=D_i/D_i^s-1$ the circumferential strain, in which $D_i^s=(1-kn)D_i^0$ is the diameter of the ith wall as an individual SWCNT with the knocked-off atom density n and D_i^0 the diameter of this SWCNT as n=0. Fitting our MD simulation results of a (10,10) SWCNT yields $E(n)=0.86-2.46n$ TPa and E_2=−1.75 TPa. These estimates agree with the recent experimental measurements: E=(1.0±0.1)

TPa and E_2=(−2.0±0.4) TPa for monolayer graphene (Lee *et al.*, 2008). Once *n* on each tube is known, we can solve D_i through minimizing Π. With k=0.75 calculated from our MD simulation, we found that our model's prediction agrees well with our MD results (see Appendix for more details).

5 Discussion

With the help of the model, we discuss some key issues regarding the fabrication of PMWCNTs using electron beam irradiation.

1. Irradiation temperature

Our MD studies revealed that the 3DB SVs generated by irradiation at room temperature in a DWCNT would lead to expansion of the tube and thus increase the interwall spacing. This expansion is undesirable for a PMWCNT. Irradiation at temperatures lower than 200 °C, therefore, should be avoided.

2. Close-cap MWCNT

In Banhart and Ajayan (1996), electron irradiation at 650 to 750 °C lead to a 35% reduction of interwall spacings in the core and 9% reduction of interwall spacings in the outer shells for carbon onions. In Sun *et al.* (2006), however, in an MWCNT filled with Fe_3C, they found only 10% reduction of the interwall spacing for the two innermost layers, 5% reduction of the interwall spacing between the second and third layers, and no measurable reduction for other shells. We believe that the much less interwall-spacing reduction of the MWCNT (Sun *et al.*, 2006) is because of the MWCNT's open structure without caps at both ends. The carbon atoms on the inner tubes are more easily displaced (Banhart *et al.*, 2005) and the interstitials between the shells can migrate away through the two open ends because of the high pressure (Sun *et al.*, 2006). It is thus reasonable to assume that the DV density of the inner tubes in an open-ended MWCNT would be higher than that of the outer tubes. As a preliminary estimate, we assume a linear dependence of *n* on tube order index *i* along the radial direction as $n(i)=n_0+(1-i/N)c_1$. Using n_0=0.04 and c_1=0.04 for a 10-walled MWCNT with an incompressible core, our model's prediction agrees well with the experimental results of Sun *et al.* (2006): the pressure exerting on the incompressible core (around 40 GPa) and the interwall spacing distribution.

For a closed structure, e.g., carbon onion, the interstitials can not migrate out of the structure but may recombine with vacancies in adjacent shells (Zaiser, 1999). Such recombination would also compensate DVs in the inner tubes of an irradiated close-cap MWCNTs, which makes the distribution of *n* different from that of the open-cap irradiated MWCNT. Thus, it is reasonable to assume a constant *n* or lower defect concentration in the inner tubes, i.e., $n(i)=n_0-(-i/N)c_2$ for a close-cap MWCNT. Fig. 3 shows the interwall spacings calculated by our model of MWCNTs with 5, 10 and 25 layers with assumed constant n=0.2, and $n(i)=0.2-0.1(1-i/N)$ for a 5-layer nanotube. In Fig. 3, it is clear that all of the interwall spacings reduce significantly and the reduction of interwall spacings between inner walls is more remarkable than that of the outer shells. This trend is consistent with the experimental observations for the closed structure: carbon onions. As a comparison, we also plot the interwall spacings of an open-cap 5-walled MWCNT with assumed $n=0.2+0.1(1-i/N)$. For all the three 5-walled MWCNTs, *n* is the same on the outermost shell and the open-cap MWCNT has the highest average *n*. It is clear that the interwall spacings of close-cap MWCNT are smaller than that of open-cap MWCNT. Thus, we can expect that the close-cap MWCNT will benefit the fabrication of the PMWCNTs.

3. Number of walls in an MWCNT

In real applications, the force is usually exerted on the outmost wall of an MWCNT. The interwall spacing between the two outmost layers is critical for the force to be effectively transferred to the inner walls. In Fig. 3, we observed that the MWCNT with the same defect density *n* but fewer walls (e.g., the 5-walled MWCNT) has more remarkable reduction in the interwall spacing between the two outmost layers. Similar results are obtained for the two linear distributions of defect density *n*. These suggest that a 5-walled MWCNT would be a better raw material for fabricating PMWCNTs than a 25-walled MWCNT.

4. Thermo-annealing

Our MD simulations show that a (10,10) SWCNT with n=0.12 DVs has a 35% loss of axial modulus and 21% loss of tensile strength. Similar degrading of tensile strength is also observed in experiment: the measured strength (about 100 GPa) of MWCNTs is about 80% of the theoretical values

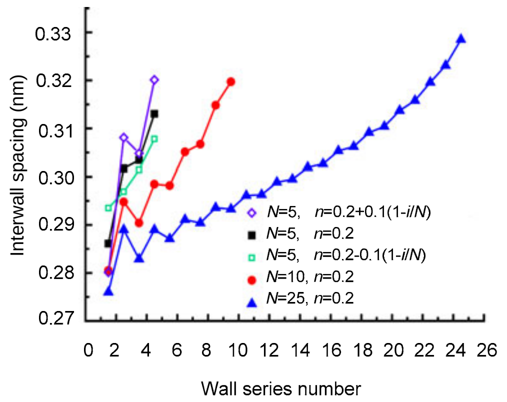

Fig. 3 Theoretical predictions (Eq. (2)) of the interwall spacings of irradiated MWCNTs with different number of walls *N* at various knocked off atom ratios *n*

(Peng *et al.*, 2008) after 30 min irradiation under 200 kV. Thermo-annealing is necessary to remove DVs and consequently recover the mechanical properties of CNTs. In experiments, most of the defects on MWCNTs could be annihilated after annealed at 1600 K in vacuum condition of 10^{-5} Torr (1 Torr =133.323 Pa) (Jung *et al.*, 2007). Our MD simulations here show that the studied 5-walled PMWCNT remains its shrunk structure under 2000 K if *n* is lower than 10%. Annealing would then recover the hexagonal wall structure of the irradiated CNTs, but with fewer atoms. Thus, the radius of annealed CNT is smaller than that of the defect-free one prior to irradiation. Our calculations show that the reduction amount of interwall spacings is close to that caused by DV. After annealing, the interwall spacings will maintain the same as the irradiated MWCNT. If the desired density of DVs exceeds the thermo-stability limit (e.g., 8% at 2000 K in our MD simulation), we can use cycles of irradiation and annealing to obtain a nearly defect-free PMWCNT with the desired mechanical properties.

6 Conclusions

In this paper, by using MD simulation, we studied the effects of three different kinds of defects (3DB SV, DV and 5-1DB SV) on the structures of SWCNTs and MWCNTs. Our MD simulations revealed that the presence of DV and 5-1DB SVs would reduce the diameters of SWCNTs, whereas 3DB SVs would increase the diameters. The coexistence of DVs and 3DB SVs can explain the controversy between our experiments and Sun *et al*. (2006)'s. We further proposed an energy model to predict the equilibrium interwall spacings of irradiated MWCNT from the defect density *n* in each wall. Based on this model and the mechanisms revealed by our MD, we provided four suggestions for fabricating PMWCNTs: (1) avoid irradiation at room temperature; (2) use close-cap MWCNTs as raw materials; (3) use MWCNTs with few walls; and, (4) use cycles of irradiation and annealing.

Acknowledgments

We thank Prof. Jin-quan WEI and Dr. Xu-chun GUI (General Research Institute for Nonferrous Metals, Beijing, China) for the fabrication of Fe_3C-filled MWCNT samples.

References

Ajayan, P.M., Ravikumar, V., Charlier, J.C., 1998. Surface reconstructions and dimensional changes in single-walled carbon nanotubes. *Physical Review Letters*, **81**(7):1437-1440. [doi:10.1103/PhysRevLett.81.1437]

Banhart, F., 1999. Irradiation effects in carbon nanostructures. *Reports on Progress in Physics*, **62**(8):1181-1221. [doi:10.1088/0034-4885/62/8/201]

Banhart, F., Ajayan, P.M., 1996. Carbon onions as nanoscopic pressure cells for diamond formation. *Nature*, **382**(6590):433-435. [doi:10.1038/382433a0]

Banhart, F., Li, J.X., Krasheninnikov, A.V., 2005. Carbon nanotubes under electron irradiation: Stability of the tubes and their action as pipes for atom transport. *Physical Review B*, **71**(24):241408. [doi:10.1103/PhysRevB.71.241408]

Cumings, J., Zettl, A., 2000. Low-friction nanoscale linear bearing realized from multiwall carbon nanotubes. *Science*, **289**(5479):602-604. [doi:10.1126/science.289.5479.602]

Ding, W., Calabri, L., Kohlhaas, K.M., Chen, X., Dikin, D.A., Ruoff, R.S., 2007. Modulus, fracture strength, and brittle vs. plastic response of the outer shell of arc-grown multi-walled carbon nanotubes. *Experimental Mechanics*, **47**(1):25-36. [doi:10.1007/s11340-006-9344-6]

Hashimoto, A., Suenaga, K., Gloter, A., Urita, K., Iijima, S., 2004. Direct evidence for atomic defects in graphene layers. *Nature*, **430**(7002):870-873. [doi:10.1038/nature02817]

Jung, S.I., Jo, S.H., Moon, H.S., Kim, J.M., Zang, D.S., Lee, C.J., 2007. Improved crystallinity of double-walled carbon nanotubes after a high-temperature thermal annealing and their enhanced field emission properties. *Journal of*

Physical Chemistry C, **111**(11):4175-4179. [doi:10.1021/jp0676078]

Krasheninnikov, A.V., Banhart, F., 2007. Engineering of nanostructured carbon materials with electron or ion beams. *Nature Materials*, **6**(10):723-733. [doi:10.1038/nmat1996]

Krasheninnikov, A.V., Lehtinen, P.O., Foster, A.S., Nieminen, R.M., 2006. Bending the rules: contrasting vacancy energetics and migration in graphite and carbon nanotubes. *Chemical Physics Letters*, **418**(1-3):132-136. [doi:10.1016/j.cplett.2005.10.106]

Krasheninnikov, A.V., Miyamoto, Y., Tomanek, D., 2007. Role of electronic excitations in ion collisions with carbon nanostructures. *Physical Review Letters*, **99**(1):016104. [doi:10.1103/PhysRevLett.99.016104]

Lee, C., Wei, X.D., Kysar, J.W., Hone, J., 2008. Measurement of the elastic properties and intrinsic strength of monolayer graphene. *Science*, **321**(5887):385-388. [doi:10.1126/science.1157996]

Lu, A.J., Pan, B.C., 2004. Nature of single vacancy in achiral carbon nanotubes. *Physical Review Letters*, **92**(10):105504. [doi:10.1103/PhysRevLett.92.105504]

Mielke, S.L., Belytschko, T., Schatz, G.C., 2007. Nanoscale fracture mechanics. *Annual Review of Physical Chemistry*, **58**(1):185-209. [doi:10.1146/annurev.physchem.58.032806.104502]

Peng, B., Locascio, M., Zapol, P., Li, S.Y., Mielke, S.L., Schatz, G.C., Espinosa, H.D., 2008. Measurements of near-ultimate strength for multiwalled carbon nanotubes and irradiation-induced crosslinking improvements. *Nature Nanotechnology*, **3**(10):626-631. [doi:10.1038/nnano.2008.211]

Plimpton, S., 1995. Fast parallel algorithms for short-range molecular-dynamics. *Journal of Computational Physics*, **117**(1):1-19. [doi:10.1006/jcph.1995.1039]

Stuart, S.J., Tutein, A.B., Harrison, J.A., 2000. A reactive potential for hydrocarbons with intermolecular interactions. *Journal of Chemical Physics*, **112**(14):6472-6486. [doi:10.1063/1.481208]

Sun, L., Banhart, F., Krasheninnikov, A.V., Rodriguez-Manzo, J.A., Terrones, M., Ajayan, P.M., 2006. Carbon nanotubes as high-pressure cylinders and nanoextruders. *Science*, **312**(5777):1199-1202. [doi:10.1126/science.1124594]

Sun, L.T., Krasheninnikov, A.V., Ahlgren, T., Nordlund, K., Banhart, F., 2008. Plastic deformation of single nanometer-sized crystals. *Physical Review Letters*, **101**(15):156101. [doi:10.1103/PhysRevLett.101.156101]

Wang, C., Wang, C.Y., 2006. Geometry and electronic properties of single vacancies in achiral carbon nanotubes. *European Physical Journal B*, **54**(2):243-247. [doi:10.1140/epjb/e2006-00448-6]

Xu, Z.P., Wang, L.F., Zheng, Q.S., 2008. Enhanced mechanical properties of prestressed multi-walled carbon nanotubes. *Small*, **4**(6):733-737. [doi:10.1002/smll.200700678]

Yu, M.F., Yakobson, B.I., Ruoff, R.S., 2000a. Controlled sliding and pullout of nested shells in individual multi-walled carbon nanotubes. *Journal of Physical Chemistry B*, **104**(37):8764-8767. [doi:10.1021/jp002828d]

Yu, M.F., Lourie, O., Dyer, M.J., Moloni, K., Kelly, T.F., Ruoff, R.S., 2000b. Strength and breaking mechanism of multiwalled carbon nanotubes under tensile load. *Science*, **287**(5453):637-640. [doi:10.1126/science.287.5453.637]

Zaiser, M., 1999. Self-compression and diamond nucleation in irradiated carbon onions: a theoretical model. *Materials Research Society Symposium Proceedings*, **540**:243-248.

Zobelli, A., Gloter, A., Ewels, C.P., Seifert, G., Colliex, C., 2007. Electron knock-on cross section of carbon and boron nitride nanotubes. *Physical Review B*, **75**(24):245402. [doi:10.1103/PhysRevB.75.245402]

Appendix

1 Fitting results of Fig. 2

Table A1 summarizes the fitting results (Eq. (1)) for the atomic structures as shown in Fig. 2

Table A1 Fitting results of Fig. 2

Atomic structure	k	D_0 (nm)
DWCNT+3DB	−0.18	1.338
DWCNT+DV	0.37	1.338
DWCNT+DV+3DB	−0.24	1.306
DWCNT+5-1DB	0.35	1.338
SWCNT+3DB	−0.21	1.336
SWCNT+DV	0.68	1.336
SWCNT+5-1DB	0.45	1.336

2 Verification of our model

In Fig. A1 we plotted the predicted interwall spacings of a 5-walled MWCNT: (5,5)@(10,10)@(15,15)@(20,20)@(25,25) with DVs of density n=0.12 in each wall. The triangles represent the results with tube-independent k=0.75 (k is actually almost independent of tube diameter except tube diameter<1.4 nm) and the circles represent the results with tube-dependent k. Both models have led to results agreeing well with those of the direct MD (black squares). For simplicity, we will adopt k=0.75 in the following discussions.

3 Specimen locating method

We located the specimen by a gradually magnification method, as shown in Fig. A2. After observed the specimen for the first time on nanoscale (Fig. A2c), we decreased the magnification and recorded the location by a digital camera. In the subsequent two observations/irradiations, we found the located specimen in the pictures of different magnifications.

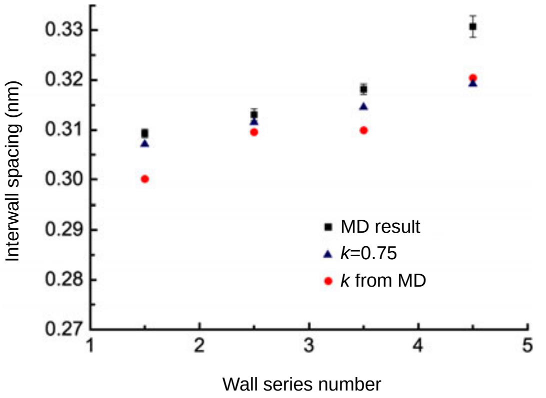

Fig. A1 Interwall spacings of a 5-walled pre-stressed (5,5)@(10,10)@(15,15)@(20,20)@(25,25) MWCNT with DVs of density *n*=0.12 in each wall

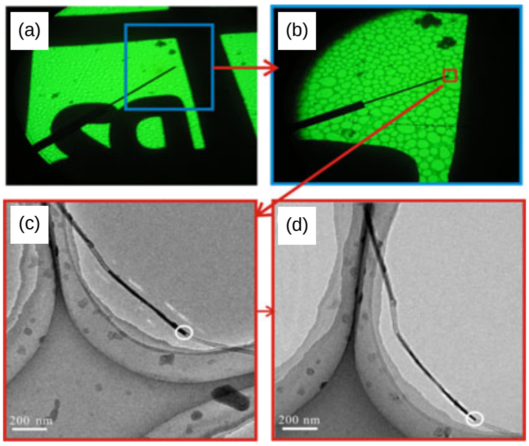

Fig. A2 Specimen locating method

(a), (b) Positions of the specimen on micrometer scale; (c) Specimen before high temperature irradiation; (d) Specimen after high temperature irradiation. The region in white circle is shown in Fig. 1